

Ab Initio Theoretical Studies on the Kinetics of the Hydrogen Abstraction Reaction of Hydroxyl Radical with CH₃CH₂OCF₂CHF₂ (HFE-374pc2)

V. Saheb*

Department of Chemistry, College of Science, Shahid Bahonar University of Kerman, Kerman, Iran

(Received 29 February 2016, Accepted 28 April 2016)

The hydrogen abstraction reaction of OH radical with CH₃CH₂OCF₂CHF₂ (HFE-374pc2) is investigated theoretically by semi-classical transition state theory. The stationary points on the potential energy surface of the reaction are located by using KMLYP density functional method along with 6-311++G(d,p) basis set. Vibrational anharmonicity coefficients, x_{ij} , required for semi-classical transition state theory calculations, are computed at the same level of theory. The geometries are re-optimized by M06-2X/6-31+G(d,p) level. Single-point energy calculations are carried out by the CBS-Q combination method. Thermal rate coefficients are computed over the temperature range 200-2000 K and they are shown to be in accordance with the available experimental data. On the basis of the computed rate coefficients, the atmospheric lifetime of HFE-374pc2 is estimated to be about 2 months.

Keywords: HFE-374pc2, Hydroxyl radical, *Ab initio*, Semi-classical transition state, Atmospheric lifetime

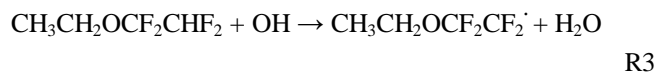
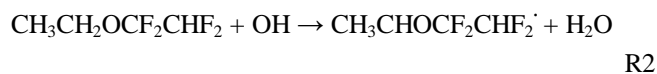
INTRODUCTION

Global warming and ozone layer depletion have become two major environmental problems over the past decades due to the emission of a diversity of halogen-containing compounds at the earth's surface and their accumulation in the atmosphere. A worldwide effort has been made to ban the stable and long-lived chlorofluorocarbons (CFC's) and replace them with the more reactive hydrogen-containing halocarbons such as hydrochlorofluorocarbons (HCFC's), hydrofluorocarbons (HFC's) and hydrofluoroethers (HFE's) [1]. The latter halocarbons have shorter atmospheric lifetimes because they undergo hydrogen-abstraction reactions with reactive atmospheric species especially OH radicals, known as atmospheric detergents. One proposed HFE as a replacement for long-lived ozone depleting substances is CH₃CH₂OCF₂CHF₂ with the commercial name of HFE-374pc2 [1].

So far, two research groups have measured the overall rate coefficient for the reaction of CH₃CH₂OCF₂CHF₂ with OH radical [2,3]. Heathfield and coworkers have employed a pulse radiolysis technique to produce OH radicals from water molecules followed by monitoring the OH radical concentration by its ultra-violet absorption and obtained a value of $4.33 \times 10^{-13} \text{ cm}^3 \text{ molecule}^{-1} \text{ s}^{-1}$ for CH₃CH₂OCF₂CHF₂ + OH [2]. On the basis of their kinetics measurements, they estimated that the atmospheric lifetime of CH₃CH₂OCF₂CHF₂ is about 0.1 year. Kinetic measurements were carried out by Tokuhashi and coworkers [3] over the temperature range 250-430 K using a flash photolysis method combined with a laser induced fluorescence technique to monitor the OH radical concentration and determined the Arrhenius rate constant expression as $k = 2.57 \times 10^{-12} \text{ cm}^3 \text{ molecule}^{-1} \text{ s}^{-1} \exp(-730/T)$. Three reaction paths can be considered for the title reaction:



*Corresponding author. E-mail: vahidsaheb@mail.uk.ac.ir



In the present research, it is attempted to employ high-level quantum chemical methods to explore important regions in potential energy surfaces (PES) of these hydrogen-abstraction reactions. Next, Semi-Classical Transition State Theory (SCTST) is used to compute the thermal rate constants for each channel. On the basis of the overall computed rate constants, an estimation on the atmospheric lifetime of HFE-374pc2 is made.

COMPUTATIONAL DETAILS

Electronic-Structure Calculations

In this research, first, the PES for OH + CH₃CH₂OCF₂CHF₂ is explored by KMLYP density functional theory (DFT) method [4] along with the standard 6-311++G(d,p) basis set to locate the structures of the stationary points, *i.e.*, reactants, van der Waals complexes, transition states and products. In the KMLYP method, the exchange functional is obtained by mixing Slater exchange and exact exchange and the correlation functional is a mix of Vosko, Wilk, Nusair (VWN) [5] and that of Lee, Yang, and Parr (LYP) correlation functionals [6]. The KMLYP hybrid density-functional method is assessed against 132 energy data, including 74 barrier heights and 58 reaction enthalpies. It is shown that the predicted reaction barrier heights by KMLYP method has the same accuracy as CBS-APNO, and transition state barriers and reaction enthalpies have smaller errors in comparison with B3LYP, BHandHLYP, and G2 [4]. The KMLYP method is used to calculate harmonic vibrational frequencies and x_{ij} vibrational anharmonicity coefficients.

The structures of the stationary points are re-optimized by M06-2X hybrid meta density functional theory (HMDFT) method [5] along with the recommended basis set 6-31+G(d,p). Various databases containing energetic data, bond lengths, vibrational frequencies and vibrational zero point energies are used to assess the performance of this HMDFT method and it is recommended for

applications involving main-group thermochemistry, kinetics and noncovalent interactions [5]. In order to compute accurate barrier heights and reaction energies, single-point energy calculations are performed with CBS-Q combination method [6] on the geometries optimized at the M06-2X/6-31+G(d,p) level of theory. The energy computed by the CBS-Q method is a combination of single point energy calculations at CCSD(T), MP4 and MP2 levels and is proved to have good accuracy for thermochemical calculations (mean absolute error of 0.87 kcal mol⁻¹). Gaussian 09 packages are used to carry out all quantum chemical calculations [7].

Dynamical Calculations

In this research, SCTST is used to compute the thermal rate constants for OH + CH₃CH₂OCF₂CHF₂ reaction. In SCTST [8-11], canonical rate constant is computed according to the following equation:

$$k(T) = \frac{1}{h} \frac{\int_0^\infty G^\ddagger(E) \exp(-E/k_B T) dE}{Q_{re}(T)} \quad (1)$$

where h is Planck's constant, k_B is Boltzmann's constant, T is the temperature, Q_{re} is the total partition function of the reactant(s), and $G^\ddagger(E)$ is the cumulative reaction probability (CRP). The rotations and vibrations of a molecule can be decoupled at moderate temperatures and the Eq. (1) is reduced to

$$k(T) = \frac{1}{h} \frac{Q_t^\ddagger Q_r^\ddagger \int_0^\infty G_v^\ddagger(E_v) \exp(-E_v/k_B T) dE_v}{Q_t Q_r Q_v(T)} \quad (2)$$

In the above equation, Q_t , Q_r and Q_v are the translational, rotational and vibrational partition functions of the reactants, respectively; and the Q_t^\ddagger and Q_r^\ddagger represent corresponding values for transition state. Integration is made over vibrational energy of transition state. The cumulative reaction probability, which is the sum of probabilistic quantum pathways leading to the product, is defined as

$$G_v^\ddagger(E_v) = \sum_{n_1} \sum_{n_2} \dots \sum_{n_{F-2}} \sum_{n_{F-1}} P_n(E_v) \quad (3)$$

The semiclassical tunneling probability, P_n , in the above equation is expressed as

$$P_n(E) = \frac{1}{1 + \exp[2\theta(n, E)]} \quad (4)$$

where $\theta(n, T)$ is the barrier penetration integral and is given by

$$\theta(n, E) = \frac{\pi \Delta E}{\Omega_F} \frac{2}{1 + \sqrt{1 + 4x_{FF} \Delta E / \Omega_F^2}} \quad (5)$$

ΔE and Ω_F , needed for computing $\theta(n, T)$, are given by the following expressions:

$$\Delta E = \Delta V_0 + \varepsilon_0 - E + \sum_{k=1}^{F-1} \omega_k \left(n_k + \frac{1}{2} \right) + \sum_{k=1}^{F-1} \sum_{l=k}^{F-1} x_{kl} \left(n_k + \frac{1}{2} \right) \left(n_l + \frac{1}{2} \right) \quad (6)$$

$$\Omega_F = \bar{\omega}_F - \sum_{k=1}^{F-1} x_{kF} \left(n_k + \frac{1}{2} \right) \quad (7)$$

$$\bar{\omega}_F = -i\omega_F \quad \text{and} \quad \bar{x}_{kF} = -ix_{kF} \quad (8)$$

In the equations 6-8, F is the number of vibrations in the transition state, ω_k is the harmonic vibrational frequency of the k_{th} vibration, ω_F is the saddle-point imaginary frequency, x_{kl} 's are the elements of the vibrational anharmonicity constants matrix for the degrees of freedom orthogonal to the reaction coordinate, x_{kF} 's are the (pure imaginary) anharmonicity constants between the reaction coordinate and the orthogonal degrees of freedom, x_{FF} is the (pure real) anharmonicity constant for the reaction path, and ΔV_0 is the classical barrier height.

SCTST formalism was developed by Miller and colleagues in 1970's and it was applicable only for the small systems because it was computationally demanding [8-11]. Recently, Barker and coworkers have developed an algorithm by which SCTST can be applied to saddle-points with more than ten atoms [12-14]. Barker *et al.* have improved the Basire *et al.* algorithm [15] and applied it for computing the density of states and cumulative reaction probabilities in chemical kinetics. Basire and coworkers have considered the vibrations as a fully coupled

anharmonic system and used a perturbation theory expansion to compute quantum density of states. The Basire *et al.* algorithm is in turn based on the Wang and Landau [16-17] algorithm which is a Monte Carlo algorithm using a random walk in energy space to obtain an accurate estimate of the density of states for classical statistical models. In the SCTST formalism, the coupling between all of the vibrational degrees of freedom including reaction coordinate are considered. Zero point energy and quantum mechanical tunneling along the curved reaction path in hyperdimensional space is also accounted for.

Barker and colleagues have developed the MULTIWELL computer program package [18] which includes the programs ADENSUM, SCTST, THERMO and some other useful programs for computing the partition functions of the reactants, the CRPs of transition states and the thermal rate constants. In this research work, rate coefficients are computed by MULTIWELL program package.

RESULTS AND DISCUSSION

On the basis of computed energies at the CBS-Q//M062/6-31G(d,p) level of theory, the mechanism of the hydrogen-abstraction reactions from $\text{CH}_3\text{CH}_2\text{OCF}_2\text{CHF}_2$ by OH radical can be described as follows. The reaction proceeds through a van der Waals complex, denoted as vdWi, with an energy of $10.41 \text{ kJ mol}^{-1}$ lower than the reactants. Next, hydrogen atoms transfer from $\text{CH}_3\text{CH}_2\text{OCF}_2\text{CHF}_2$ to OH radicals through the transition state structures TS1, TS2 and TS3 leading to van der Waals complexes vdWf1, vdWf2 and vdWf3, respectively. The energies of the transition states TS1, TS2 and TS3 relative to reactants are 6.41, -0.63 and $13.61 \text{ kJ mol}^{-1}$, respectively. In the latter van der Waals complexes, water molecules are attached to the produced radicals via weak interactions. The relative energies of the complexes vdWf1, vdWf2 and vdWf3 are -96.88, -98.33 and $-85.04 \text{ kJ mol}^{-1}$. The products of relevant complexes are $\text{CH}_2\text{CH}_2\text{OCF}_2\text{CHF}_2 + \text{H}_2\text{O}$ (P1), $\text{CH}_3\text{CHO CF}_2\text{CHF}_2 + \text{H}_2\text{O}$ (P2) and $\text{CH}_3\text{CH}_2\text{OCF}_2\text{CF}_2 + \text{H}_2\text{O}$ (P3), respectively. The products P1, P2 and P3 are 67.22, 85.94 and $64.65 \text{ kJ mol}^{-1}$ more stable than the reactants, respectively. The potential energy profile of the reaction is depicted in Fig. 1. It shows the relative energies

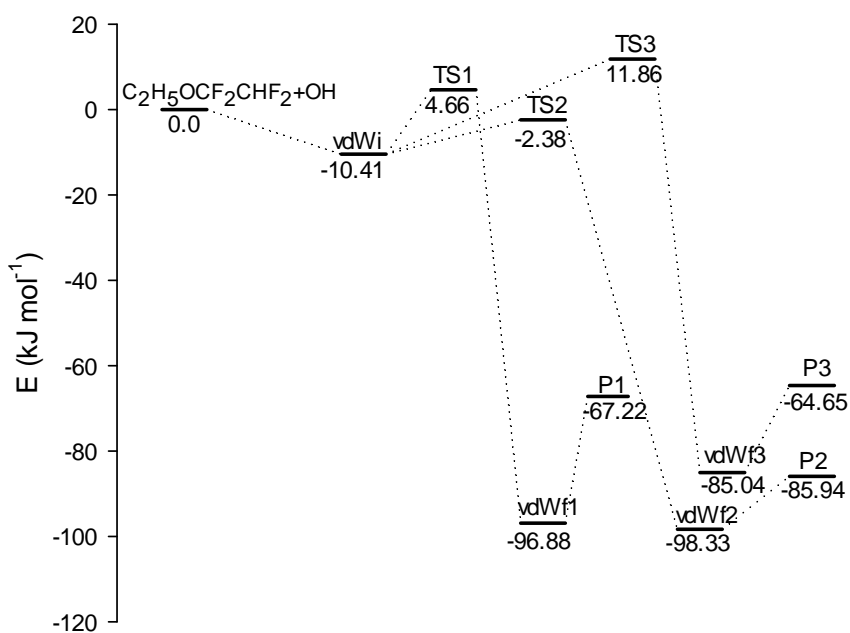


Fig. 1. Relative energies of the stationary points located on the doublet ground-state potential energy surface of the $\text{CH}_3\text{CH}_2\text{OCF}_2\text{CHF}_2 + \text{OH}$ reaction. The energy values are given in kJ mol^{-1} and are calculated using CBS-Q/M06-2X theory.

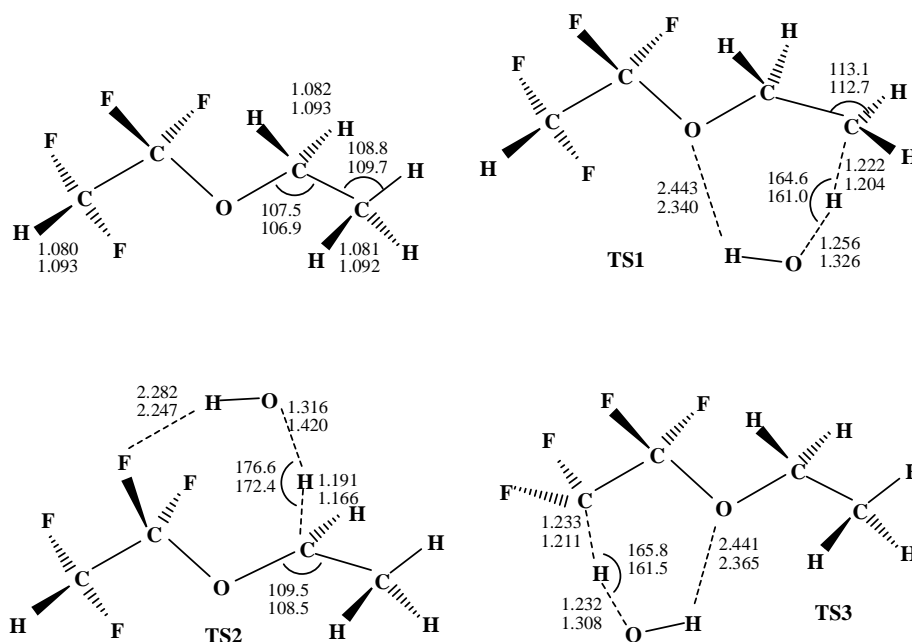


Fig. 2. The geometries of the reactant and transition states for the reaction paths R1, R2 and R3, calculated at the KMLYP/6-311++G(d,p) (top values) and M06-2X/6-31+G(d,p) (bottom values).

of the species arising from the reaction $\text{OH} + \text{CH}_3\text{CH}_2\text{OCF}_2\text{CHF}_2$. The ΔH for the reaction channels R1, R2 and R3 are found to be -63.54, -82.40 and -61.44 kJ mol^{-1} , respectively. It shows that the reaction $\text{OH} + \text{CH}_3\text{CH}_2\text{OCF}_2\text{CHF}_2$ is an exothermic process.

The geometries of reactant, van der Waals complexes

and transition states are shown in Fig. 2. The corresponding z-matrices are given in the Supplemental Information. The principal moments of inertia and the harmonic vibrational frequencies of the reactants and transition states, calculated at the KMLYP/6-311++G(d,p) level of theory, are given in Table 1. The anharmonicity constant matrices for the

Table 1. Vibrational Wave Numbers and Moments of Inertia I_i for the Reactant and Transition States of the Reactions R1, R2 and R3 Calculated with KMLYP/6-311++G(d,p)

| | The vibrational frequencies (cm^{-1}) | The principal moments of inertia (amu \AA^2) |
|--|--|---|
| $\text{CH}_3\text{CH}_2\text{OCF}_2\text{CHF}_2$ | 3260.0,3254.3,3251.0,3231.9,3183.2,3166.9,1592.1, 1562.9,1558.8,1541.8,1508.0,1466.3,1451.1,1387.1, 1377.7,1364.6,1254.8,1241.1,1238.8,1217.2,1181.9, 1136.6,977.4,910.1,857.7,827.2,644.4,612.1,569.4, 442.9,389.5,356.6,281.4,264.4,248.9, <u>134.2,105.6,73.7,45.5</u> | 169.9266,477.9314,543.5296 |
| TS1 | 1734.7i,3979.9,3301.9,3254.2,3236.5,3215.4,3171.2, 1577.1,1557.5,1520.9,1502.9,1482.7,1453.3,1389.0, 1366.8,1356.8,1309.5,1258.6,1241.5,1225.0,1210.4, 1188.8,1136.1,984.7,950.9,902.5,881.4,825.0,683.5, 638.4,609.7,569.8,447.8,419.6,389.1,355.0,314.4,279 .0,248.9,165.0,131.4, <u>114.1,78.4,46.8,26.2</u> | 259.8540,601.1399,752.3667 |
| TS2 | 1330.0i,3992.9,3264.5,3254.7,3244.8,3227.1,3161.8, 1556.7,1550.5,1535.5,1509.9,1466.1,1452.2,1420.4, 1406.6,1391.1,1364.3,1259.0,1244.0,1218.9,1207.5, 1181.3,1176.0,997.8,940.3,913.8,835.5,811.7,685.0, 641.6,610.7,571.9,442.4,387.1,361.8,283.0,259.0, 248.7,228.9,164.4,126.6, <u>120.7,101.4,63.5,28.9</u> | 247.5185,615.5105,741.0770 |
| TS3 | 1924.5i,3979.3,3260.2,3251.6,3235.3,3187.3,3166.2, 1591.7,1567.5,1560.3,1543.0,1513.0,1476.4,1464.7, 1379.3,1360.1,1342.0,1280.4,1254.0,1239.0,1190.1, 1182.4,1131.6,1003.8,956.1,877.1,856.1,799.6,663.6, 631.1,580.7,453.4,418.8,393.3, 352.7,286.7,264.7,263.1,249.0,148.1,122.3, <u>101.3,</u> <u>85.4,59.7,31.9</u> | 296.8848,538.6320,632.4851 |

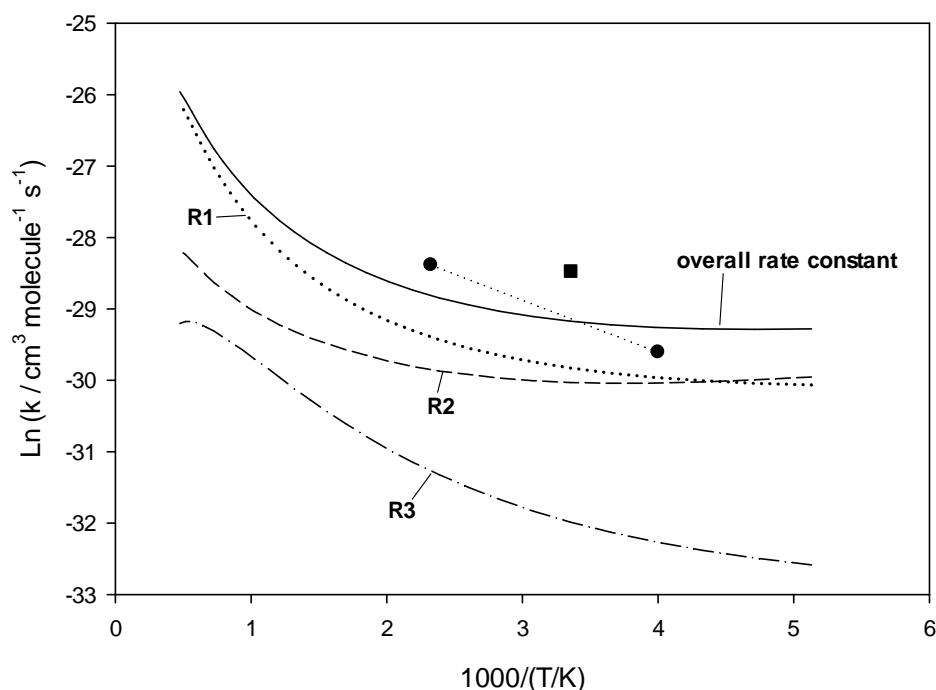


Fig. 3. The computed rate coefficients for the reaction channels R1 (dotted line), R2 (dash line), R3 (dash-Dotted line) and the overall rate constant (solid line) over the temperature range 200-2000 K. Experimental data are given for the purpose of comparison. (●) from Ref. [2], (■) from Ref. [3].

transition states TS1, TS2 and TS3 computed by KMLYP method are provided in the Supplemental Information (Table 2S to 4S). The low vibrational frequencies in the $\text{CH}_3\text{CH}_2\text{OCF}_2\text{CHF}_2$ and transition states (underlined in Table 2) corresponds to hindered internal rotations along C-C and C-O bonds. It is attempted to compute the sum of states for these degrees of freedom, by employing the ro-vibrational G matrix-based algorithm of Harthcock *et al.* [19] for the effective reduced masses for one-dimensional torsions. However, it is found that the low-vibrational frequencies correspond to very similar motions in the $\text{CH}_3\text{CH}_2\text{OCF}_2\text{CHF}_2$ and the transition states of the reactions R1, R2 and R3 and their corresponding partition function cancel from the numerator and denominator of the Eq. (2).

Having the barrier heights, the principal moments of inertia, the harmonic vibrational frequencies and anharmonicity constant matrices for the transition states TS1, TS2 and TS3, the corresponding CRP's are calculated according to Eqs. (3) to (8) employing SCTST program in MULTIWELL. Next, having the principal moments of inertia and the harmonic vibrational frequencies of the

reactants, the thermal rate coefficients for the reaction paths R1, R2 and R3 are computed by THERMO over the temperature range 200-2000 K. The computed rate coefficients for the reaction channels R1, R2, R3, the overall rate coefficient and the available experimental data are shown in Fig. 3. It is revealed that the computed rate constants are in more agreement with the experimental data of Heathfield and coworkers [2]. Nonetheless, the present theoretical results predict a slightly lower activation energy in comparison with the latter experimental data.

Regarding the atmospheric implications, the lifetime of the HFE-374pc2 could be estimated via the overall rate constant for the reaction HFE-374pc2 with OH radicals at 272 K. The rate constant at 272 K and tropospheric lifetime of CH_3CCl_3 are usually considered as benchmark quantities for estimating the lifetime of atmospherically important compounds [20]. The lifetime of the HFE-374pc2 is obtained by the following equation:

$$\tau_{\text{HFE-374pc2}} = \frac{k_{\text{CH}_3\text{CCl}_3}}{k_{\text{HFE-374pc2}}} \tau_{\text{CH}_3\text{CCl}_3}$$

$k_{CH_3CCl_3}$ and $k_{HFE-374pc2}$ are the rate coefficients for the reactions of CH_3CCl_3 and HFE,374pc2 with OH radicals at 272 K, respectively. $\tau_{CH_3CCl_3}$ and $\tau_{HFE-374pc2}$ are the tropospheric lifetimes of CH_3CCl_3 and HFE-374pc2, respectively. The literature values for $k_{CH_3CCl_3}$ at 272 K and $\tau_{CH_3CCl_3}$ are $6.0 \times 10^{-15} \text{ cm}^3 \text{ molecule}^{-1} \text{ s}^{-1}$ [21] and 5.99 years [22], respectively. According to the present calculations, the lifetime of HFE-374pc2 is estimated to be about 2 months.

Finally, it is attempted to show the temperature dependence of overall reaction by the following four-parameter equation proposed by Zheng and Truhlar [23]:

$$k(T) = A (T/K)^n \exp\left[\frac{-E(T+T_0)}{T^2+T_0^2}\right] \quad (11)$$

Therefore, the computed rate constants for the overall reaction is fitted to the Eq. (11) and for the temperature range 200-2000 K, the parameters A , n , E and T_0 are found to be $1.81 \times 10^{-14} \text{ cm}^3 \text{ molecule}^{-1} \text{ s}^{-1}$, 0.75, 885.6 K and 610.5 K, respectively.

CONCLUSIONS

In this research, the rate coefficients for the H-abstraction reaction of HFE-374pc2 with hydroxyl radical is computed by SCTST. The energies and other molecular properties of the stationary points on the potential energy surface of the reaction is computed by using high-level electronic structure theories. The geometry optimizations, and calculations of vibrational frequencies and vibrational anharmonicity constants are performed at the KMLYP/6-311++G(d,p) level of theory. Better estimations of the barrier heights of the reaction path are obtained by single-point energy calculations at the CBS-Q level of theory on the optimized geometries at the M06-2X/6-31+G(d,p) level. The calculated rate constants are in good agreement with the available experimental data. On the basis of the present calculations, the lifetime of HFE-374pc2 is estimated to be about 2 months.

REFERENCES

[1] World Meteorological Organization (WMO), *Scientific Assessment of Ozone Depletion: 2014*,

World Meteorological Organization, Global Ozone Research and Monitoring Project-Report No. 55, Geneva, Switzerland: **2014**.

[2] Heathfield, A. E.; Anastasi, C.; Pagsberg, P. B.; McCulloch, A., Atmospheric lifetimes of selected fluorinated ether compounds. *Atmos. Environ.*, **1998**, *32*, 711-717, DOI: 10.1016/S1352-2310(97)00330-0.

[3] Tokuhashi, K.; Takuhashi, A.; Kaise, M.; Kondo, S., Rate constants for the reactions of OH radicals with CH_3OCF_2CHFCl , CHF_2OCF_2CHFCl , $CHF_2OCHClCF_3$, and $CH_3CH_2OCF_2CHF_2$. *J. Geophys. Res.*, **1999**, *104*, 18681-18688, DOI: 10.1029/1999JD900278.

[4] Kang, J. K.; Musgrave, C. B., Prediction of transition state barriers and enthalpies of reaction by a new hybrid density-functional approximation. *J. Chem. Phys.*, **2001**, *115*, 11040-11051, DOI: 10.1063/1.1415079.

[5] Vosko, S. H.; Wilk, L.; Nusair, M., Accurate spin-dependent electron liquid correlation energies for local spin density calculations: A critical analysis. *Can. J. Phys.*, **1980**, *58*, 1200-1211, DOI: 10.1139/p80-159.

[6] Lee, C.; Yang, W.; Parr, R. G., Development of the colle-salvetti correlation-energy formula into a functional of the electron density. *Phys. Rev. B*, **1988**, *37*, 785-789, DOI: 10.1103/PhysRevB.37.785.

[7] Zhao, Y.; Truhlar, D. G., The M06 suite of density functionals for main group thermochemistry, thermochemical kinetics, noncovalent interactions, excited states, and transition elements: Two new functionals and systematic testing of four M06-class functionals and 12 other functional. *Theory Chem. Acc.*, **2008**, *120*, 215-241, DOI: 10.1007/s00214-007-0310-x.

[8] Montgomery, Jr., J. A.; Frisch, M. J.; Ochterski, J. W.; Petersson, G. A., A complete basis set model chemistry. VI. use of density functional geometries and frequencies. *J. Chem. Phys.*, **1999**, *110*, 2822-2827, DOI: 10.1063/1.477924.

[9] Gaussian 09, Revision A.1, Frisch, M. J.; Trucks, G. W.; Schlegel, H. B.; Scuseria, G. E.; Robb, M. A.; Cheeseman, J. R.; Scalmani, G.; Barone, V.; Mennucci, B.; Petersson, G. A.; Nakatsuji, H.;

- Caricato, M.; Li, X.; Hratchian, H. P.; Izmaylov, A. F.; Bloino, J.; Zheng, G.; Sonnenberg, J. L.; Hada, M.; Ehara, M.; Toyota, K.; Fukuda, R.; Hasegawa, J.; Ishida, M.; Nakajima, T.; Honda, Y.; Kitao, O.; Nakai, H.; Vreven, T.; Montgomery, J. A., Jr.; Peralta, J. E.; Ogliaro, F.; Bearpark, M.; Heyd, J. J.; Brothers, E.; Kudin, K. N.; Staroverov, V. N.; Kobayashi, R.; Normand, J.; Raghavachari, K.; Rendell, A.; Burant, J. C.; Iyengar, S. S.; Tomasi, J.; Cossi, M.; Rega, N.; Millam, J. M.; Klene, M.; Knox, J. E.; Cross, J. B.; Bakken, V.; Adamo, C.; Jaramillo, J.; Gomperts, R.; Stratmann, R. E.; Yazyev, O.; Austin, A. J.; Cammi, R.; Pomelli, C.; Ochterski, J. W.; Martin, R. L.; Morokuma, K.; Zakrzewski, V. G.; Voth, G. A.; Salvador, P.; Dannenberg, J. J.; Dapprich, S.; Daniels, A. D.; Farkas, Ö.; Foresman, J. B.; Ortiz, J. V.; Cioslowski, J.; Fox, D. J. Gaussian, Inc., Wallingford CT, **2009**.
- [10] Miller, W. H., Semiclassical limit of quantum mechanical transition state theory for nonseparable systems. *J. Chem. Phys.*, **1975**, *62*, 1899-1906; DOI: 10.1063/1.430676.
- [11] Miller, W. H., Semi-classical theory for non-separable systems: Construction of "Good" action-angle variables for reaction rate constants. *Faraday Discuss. Chem. Soc.*, **1977**, *62*, 40-46, DOI: 10.1039/DC9776200040.
- [12] Miller, W. H.; Hernandez, R.; Handy, N. C.; Jayatilaka D.; Willets, A., *Ab Initio* calculation of anharmonic constants for a transition state, with application to semiclassical transition state tunneling probabilities. *Chem. Phys. Lett.*, **1990**, *172*, 62-68, DOI: 10.1016/0009-2614(90)87217-F.
- [13] Hernandez, R.; Miller, W. H., Semiclassical transition state theory. A new perspective. *Chem. Phys. Lett.*, **1993**, *214*, 129-136, DOI: 10.1016/0009-2614(93)90071-8.
- [14] Nguyen, T. L.; Barker, J. R., Sums and densities of fully coupled anharmonic vibrational states: A comparison of three practical methods. *J. Phys. Chem. A*, **2010**, *114*, 3718-3730, DOI: 10.1021/jp100132s.
- [15] Nguyen, T. L.; Stanton J. F.; Barker, J. R., A practical implementation of semi-classical transition state theory for polyatomics. *Chem. Phys. Lett.*, **2010**, *499*, 9-15, DOI: 10.1016/j.cplett.2010.09.015.
- [16] Nguyen, T. L.; Stanton J. F.; Barker, J. R., *Ab Initio* reaction rate constants computed using semiclassical transition-state theory: $\text{HO} + \text{H}_2 \rightarrow \text{H}_2\text{O} + \text{H}$ and isotopologues. *J. Phys. Chem. A*, **2011**, *115*, 5118-5126, DOI: 10.1021/jp2022743.
- [17] Basire, M.; Parneix P.; Calvo, F. J., Quantum anharmonic densities of states using the Wang-Landau method. *J. Chem. Phys.*, **2008**, *129*, 081101, DOI: 10.1063/1.2965905.
- [18] Wang, F.; Landau, D. P., Efficient, multiple-range random-walk algorithm to calculate the density of states. *Phys. Rev. Lett.*, **2001**, *86*, 2050-2053, DOI: 10.1103/PhysRevLett.86.2050 .
- [19] Wang, F.; Landau, D. P., Determining the density of states for classical statistical models: A random walk algorithm to produce a flat histogram. *Phys. Rev. E*, **2001**, *64*, 56101, DOI: 10.1103/PhysRevE.64.056101.
- [20] Barker, J. R.; Ortiz, N. F.; Preses, J. M.; Lohr, L. L.; Maranzana, A.; Stimac, P. J.; Nguyen, T. L.; Kumar, T. J. D., MultiWell-2014.1 Software; Barker, J. R., Ed.; University of Michigan: Ann Arbor, Michigan, U.S.A., 2014; <http://aoss.engin.umich.edu/multiwell/>.
- [21] Harthcock, M. A.; Laane, J., Calculation of two-dimensional vibrational potential energy surfaces utilizing prediagonalized basis sets and Van Vleck perturbation methods. *J. Phys. Chem.*, **1985**, *89*, 4231-4240, DOI: 10.1021/j100266a017.
- [22] Chen, L.; Tokuhashi, K.; Kutsuna, S.; Sekia, A., Rate constants for the gas-phase reaction of $\text{CF}_3\text{CF}_2\text{CF}_2\text{CF}_2\text{CHF}_2$ with OH radicals at 250-430 K. *Int. J. Chem. Kinet.*, **2004**, *36*, 26-33, DOI: 10.1002/kin.10170.
- [23] Kurylo, M. J.; Orkin, V. L., Determination of atmospheric lifetimes *via* the measurement of OH radical kinetics. *Chem. Rev.*, **2003**, *103*, 5049-5076, DOI: 10.1021/cr020524c.
- [24] Prinn, R. G.; Huang, J.; Weiss, R. F.; Cunnold, D. M.; Fraser, P. J.; Simmonds, P. G.; McCulloch, A.; Harth, C.; Salameh, P.; O'Doherty, S.; Wang, R. H. J.; Porter, L.; Miller, B. R., Evidence for substantial variations of atmospheric hydroxyl radicals in the past

two decades. *Science*, **2001**, 292, 1882-1888, DOI: 10.1126/science.1058673.

[25] Zheng, J.; Truhlar, D. G., Kinetics of hydrogen-

transfer isomerizations of butoxyl radicals. *Phys. Chem. Chem. Phys.*, **2010**, 12, 7782-7793, DOI: 10.1039/B927504E.